water

MDPI

Article

Study on the Evaporation Suppression Efficiency and Optimal Diameter of Plain Reservoirs Covered by EPS Floating Balls in Arid Areas

Buzhi Wang [1], Kebin Shi [1,*], Guangliang Zhang [2], Siyuan Xu [1] and Jiangtao Wang [3]

1 School of Water Resources and Civil Engineering, Xinjiang Agricultural University, Urumqi 830052, China; wangbuzhi@foxmail.com (B.W.)
2 Xinjiang Fukang Pumped Storage Co., Ltd., Fukang 831500, China
3 Heigou Basin Management Station, Water Resources Bureau, Gaochang District, Turpan 838000, China
* Correspondence: xndsg@sina.com

Abstract: Current research on the evaporation inhibition effect of polyethylene (PE) floats has been relatively comprehensive, and the cost is relatively high when it is arranged in remote mountainous areas. In order to find a more economical anti-evaporation material, five kinds of solid expanded polystyrene (EPS) floating balls with different diameters of 10 mm, 40 mm, 80 mm, 120 mm and 150 mm were selected to study the evaporation suppression efficiency (ESE) of EPS floating balls on the evaporation of reservoir water surfaces in arid areas. The outdoor evaporator test and the wind wave test in the reservoir area were carried out. Combined with various meteorological data, the evaporation inhibition rates of EPS floating balls with different diameters during a non-freezing period were calculated. The durability, seepage prevention, wind resistance, frost resistance, aging resistance and other properties of EPS were observed under different climatic conditions. In the evaporator test, the relationship between the diameter of the floating balls and the ESE was not a single function. The ESE of floating balls with a diameter of 40 mm was the highest, at 76.31%. In the wind wave test in the reservoir area, the ESE of the 10 mm floating balls was the lowest, at 34.79%, and the ESEs of the other four diameters of EPS floating balls were above 85% and positively related to the diameter of the floating balls. The test further improved the selection scheme for the diameter of the anti-evaporation floating balls, provided a reference for the practical application of EPS floating balls in future water-saving projects in the reservoir area, and enriched the content of water-saving projects for plain reservoirs in arid areas.

Keywords: EPS float ball; water saving; arid area; evaporation suppression efficiency; expanded polystyrene

Citation: Wang, B.; Shi, K.; Zhang, G.; Xu, S.; Wang, J. Study on the Evaporation Suppression Efficiency and Optimal Diameter of Plain Reservoirs Covered by EPS Floating Balls in Arid Areas. *Water* **2023**, *15*, 1047. https://doi.org/10.3390/w15061047

Academic Editor: Athanasios Loukas

Received: 19 February 2023
Revised: 7 March 2023
Accepted: 7 March 2023
Published: 9 March 2023

1. Introduction

1.1. Background

The northwest of China has a high altitude and is deep inland. It takes ice and snow meltwater and groundwater as its main water sources. The precipitation season has obvious characteristics, and the dry and wet seasons are distinct. The meteorological characteristics include high wind speed and low humidity, leading to high annual evaporation [1]. This area has become one of the regions with the greatest shortages of water resources in China. Taking Xinjiang as an example, 1/6 of the land area only accounts for 3% of China's water resources, while plain reservoirs account for a high proportion. Significant evaporation greatly reduces the utilization rate of water resources in reservoirs. The water loss of the plain reservoir in Xinjiang is about 34.1×10^8 m^3 per year, due to a leakage and evaporation, while the evaporation of water is about 26.1×10^8 m^3, accounting for 77% of the total loss [2]. Unfortunately, this number will continue to increase [3].

Currently, the problems brought on by the development of agriculture in China are becoming increasingly prominent [4]. Due to unreasonable agricultural irrigation and imperfect water conservancy facilities in some areas, various water conservancy facilities are constantly damaged, and damaged for long-term use; updates and maintenance are not timely enough, resulting in large water losses in the process of water transmission and the low efficiency of agricultural irrigation practices [5]. Although China's water-saving irrigation area has increased significantly in recent years, the proportion of farmland water-saving irrigation area is far from meeting the requirements of efficient water conservation [6].

From a global perspective, it is estimated that the evaporation loss from reservoirs will be greater than the consumption of industrial and domestic water [7]. With the vigorous promotion and popularization of agricultural water saving, the importance of reservoir evaporation prevention research in water-saving projects has become prominent, especially in arid areas [8], and water saving in reservoir areas is expected to become an important way to solve the shortage of water resources.

1.2. Research Status

Currently, a considerable number of scholars are committed to exploring the application of floating photovoltaic (FPV) systems on water surfaces [9–11]. This is a very unique idea, and the results are also quite remarkable. However, it is crucial to determine whether small local reservoirs can bear the cost of installation and maintenance in remote and arid areas. While protecting water resources, local economic conditions should be taken into account, and relatively cheap materials should be used to create more benefits. For example, Maritza, L.A.J. studied the reduction effect of PET bottles on water surface evaporation and achieved a 38.61% decrease in evaporation [12].

The research on evaporation prevention of plain reservoirs needs to solve two key issues: technical reliability and economic feasibility. A physical floating cover mainly inhibits evaporation by blocking the transmission of solar radiation. The anti-evaporation effect is related to the material, shape, coverage rate and other factors of the cover. There are many research contents about the influence of floating ball parameters on the inhibition of water surface evaporation [13,14]. M.M. Shalaby [15] and others suggested that farmland irrigation reservoirs should be completely covered with plastic or foam plate in order to achieve the maximum ESE (96%) in the outdoor ring anti-evaporation test. However, in multipurpose reservoirs, the impact of such projects on the ecological environment cannot be ignored. It was recommended to use white inflatable PE balls to cover reservoir surfaces, but only 90 mm diameter floating balls were used for the test. Han, K.-W. also believes that floating balls with arc structures are more suitable as an anti-evaporation material. The first large-area floating ball coverage test in China was carried out using high-density polyethylene (HDPE) floating balls, and the annual water saving rate per unit area of water area was 64.21–70.96%. He also proposed a practical application plan. However, the project investment payback period is long, and the measurement method of the floating ball wet ratio (WR) in the test process can easily result in large errors.

1.3. Research Objectives

To sum up, in view of the shortcomings of the current research on anti-evaporation floats, this test used the more economical white expanded polystyrene (EPS) solid floats. Referring to the existing research methods and research theories, five floats with different diameters (10 mm, 40 mm, 80 mm, 120 mm, 150 mm) were selected to observe the working performance of EPS floats in wind and waves. The wind speed data were recorded and processed on an hourly scale, the WR of the floating ball was calculated more accurately using the dye marking method, and the ESE of the floating ball of each diameter during the non-freezing period was calculated. The feasibility of the EPS floating ball as an anti-evaporation floating ball in plain reservoirs in arid and semi-arid areas was explored, providing a new reference scheme for anti-evaporation and water saving in plain reservoirs in arid and semi-arid areas.

2. Test Materials and Methods

2.1. General Situation of Test Area

Located in the Xinjiang Uygur Autonomous Region, Turpan Basin is the lowest basin in the world. The warm temperate desert climate makes this region a typical severe arid area in the northwest. It is surrounded by mountains, gravel Gobi, and sparse vegetation. The summer sunshine lasts more than 15 h. It is extremely dry and hot. According to meteorological station data (station No. 515730) provided by the Turpan Meteorological Bureau, the multi-year average temperature from 1957 to 2021 was 15.18 °C; average annual maximum temperature: 25.41 °C; average annual minimum temperature: 8.71 °C. The annual effective accumulated temperature above 10 °C is above 5300 °C. In the precipitation data from 1981 to 2021, the average annual precipitation was only 15.66 mm [16].

In order to simulate the climatic conditions of the reservoir, the outdoor evaporator test was carried out at Shengjintai Reservoir in Shengjin Township, Gaochang District, Turpan City, with geographical coordinates of 89°37′30″ E and 42°56′30″ N. The catchment area of the reservoir is 316,000 m^2, the control basin area above the reservoir is 88.9 km^2, the normal pool level of the reservoir is 100.5 m, the dead water level is 94.5 m, and the total storage capacity is 1,186,600 m^3.

The wind wave test was carried out in the Phase III water and soil conservation reservoir (Figure 1), about 5 km away from the downstream of the Shengjintai Reservoir, which is located in Shengjin Township, Turpan City. It is a small silting dam reservoir. The right side of the dam is connected with the drainage channel, which mainly supplies water to the downstream Erpu Township and Sanpu Township, with significant benefits of silt retention and siltation. The geographic coordinates are 89°35′13″ E and 42°56′7″ N.

Figure 1. Geographic location of the reservoir in the test area. (**a**) Shengjintai Reservoir; (**b**) Shengjintai Phase III water and soil conservation reservoir.

2.2. Selection of Test Materials

With regard to the material selection for the anti-evaporation floating balls, the ideal covering material should have low short-wave (solar radiation) absorption rate, and is usually thermal insulation material. Currently, the materials used for heat insulation in the market are mostly various foam products, and the commonly used foam types are mainly EPS, polyurethane foam (PUF), ethylene vinyl acetate copolymer foam (EVA), etc. The selected materials must meet the characteristics of appropriate density, sufficient strength, hydrophobicity, non-toxicity, freeze–thaw resistance and strong ultraviolet resistance, and must also be stable [17]. Among the current heat insulation materials, EPS foam has the characteristics of having a micro-closed cell structure [18,19] and being colorless, non-toxic, and odorless, which can prevent the material from producing toxins under long-term coverage of water surfaces with high light transmittance; the material must also be harmless to aquatic animals and plants. The thermal deformation temperature must be high, as must the surface hardness; it must not easily be damaged under the action of external forces such as wind, waves, and collisions. It must have certain antioxidant capacities, good durability, and extremely low water absorption. Acid- and alkali-resistant media [20], which do not corrode and oxidize in saline water, have a long service life and give greater play to the anti-evaporation benefits. The density of the solid EPS floating balls (Figure 2) used in this test was 18 kg/m^3, the embrittlement temperature was about −30 °C, the softening temperature was above 80 °C, the melting temperature was about 150 °C, the water absorption was 0.03–0.2, the light transmittance was nearly 90%, and the refractive index was 1.59–1.60.

Figure 2. The EPS float balls used in testing.

2.3. Test Principle

It is a complex interdisciplinary problem to physically cover the water surface to suppress the ineffective evaporation of a water body; water conservancy engineering, climatology, statistics, and engineering economics are involved, and also rich physical disciplines such as hydrodynamics, aerodynamics, and materials science.

There are four main factors affecting the evaporation rate of a natural water surface: the water body (volume, surface area and shape, water temperature, etc.), heat source (solar radiation and earth radiation), saturated water vapor pressure difference, surface wind speed, and turbulent diffusion intensity. After the anti-evaporation floating balls were laid on the open water surface, they affected the energy exchange process between the water body and the atmosphere, changed the microclimate at a certain height above the water surface, and changed the main factors affecting the evaporation rate of the water body (Figure 3). Feng, Q. [21] analyzed several factors affecting the evaporation of large water bodies in Xinjiang by analyzing the evaporation data of several major stations in Xinjiang; it was found that the effect of temperature on the evaporation of water surfaces in Xinjiang is weaker than that of solar radiation and wind speed.

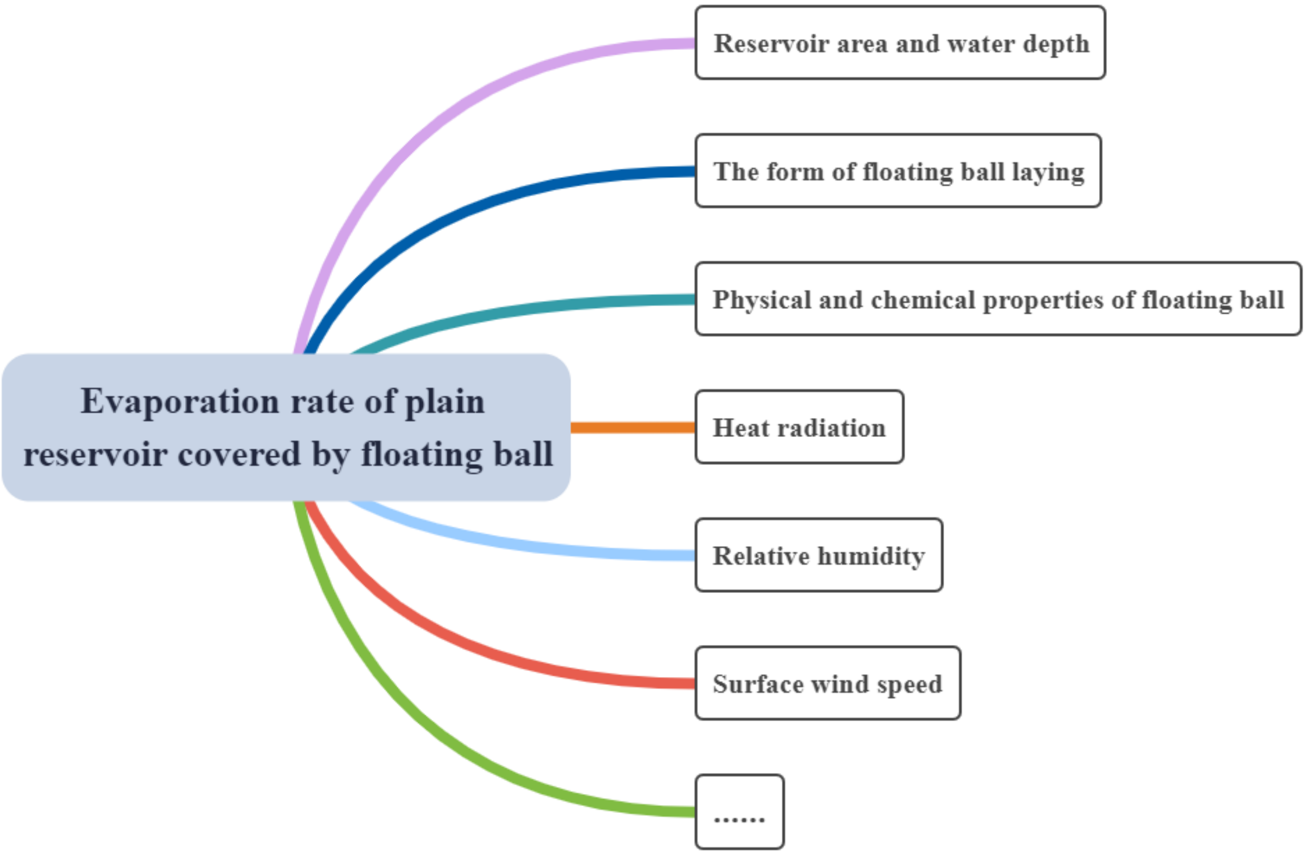

Figure 3. Main influencing factors of evaporation rate of plain reservoir covered by floating balls. Note: "......" indicates other factors affecting evaporation rate in small-sized water bodies, but their importance is weaker in reservoirs.

Through the outdoor evaporator test, we calculated the evaporation inhibition rate of floating balls of various diameters, without the influence of wind and waves, and the average evaporation inhibition rate of evaporator covered by floating balls during the non-freezing period. Through the wind wave test in the reservoir area, the wetting rate of the floating balls under different wind speeds was calculated, and the average evaporation inhibition rates of the floating balls of each diameter in the reservoir were obtained; the best anti-evaporation floating ball diameter was determined.

3. Site Layout

3.1. Outdoor Evaporator Test Layout

The outdoor evaporator test was carried out at the Shengjintai Reservoir (Figure 1a). Under the same natural conditions, six cylindrical rubber drums were used as evaporators for the outdoor tests. At present, evaporation is mainly observed through a φ 20 evaporator dish, an E-601B evaporator, and other evaporimeters of different types. Since the installation of the E-601B evaporator was complex, and at least six evaporators were required for this experiment; a cylindrical evaporator with a simpler structure and convenient installation was selected and set on site, with the φ 20 cm evaporating dish used as the evaporation control. The evaporator had a diameter of 1.2 m, a height of 0.8 m, and a wall thickness of 4.5 mm. After being filled with water, the can body remained as a cylinder without deformation. Three layers of asbestos were wrapped tightly around the outside of the rubber barrel to reduce the thermal conductivity, a 100 mm polyurethane foam (PUF) pad was placed at the bottom of the rubber barrel to isolate the surface heat, and a level meter was used to adjust the evaporator and the ground level. Before the test, the tightness of the evaporator was tested to ensure that water loss during the test could be avoided, minimizing the test error. Two rain gauges were arranged onsite to measure the rainfall during the test. In order to eliminate the impact of rainfall, the reading of the rain gauge was subtracted from the daily evaporation loss. During the hydrostatic evaporation test, the water source was extracted from the surface, middle, and bottom layers of water in the reservoir, and filled with six evaporators to the same water level. Floating balls of different diameters were placed on the water surface. See Table 1 for the measured coverage of each evaporator, and Figure 4 for the site layout, where D is the diameter of the EPS floating balls, in mm; C_1 is the evaporator test coverage, in %.

Table 1. Evaporator test design.

Number	1	2	3	4	5	6
Filler			EPS			No Coverage
D (mm)	10	40	80	120	150	-
C_1 (%)	88.2	86.1	84.5	83.4	83.2	0

Figure 4. Evaporator test site and setup layout.

3.2. Wind and Wave Test Layout

The wind and wave test was carried out on the site of the Shengjintai water and soil conservation phase iii reservoir (Figure 1b). Two materials were laid out, the HDPE buoyancy tanks and the floating balls. The HDPE buoyancy tank was connected in series as a fence, and the five diameters of floating balls were filled separately (Figure 5). When filling, the coverage rate was as close as possible to 91% without stacking. The measured coverage rate is shown in Table 2. Dyed floating balls (Section 5.2) scattered in the fence were used to calculate the WR of floating balls during the statistical period.

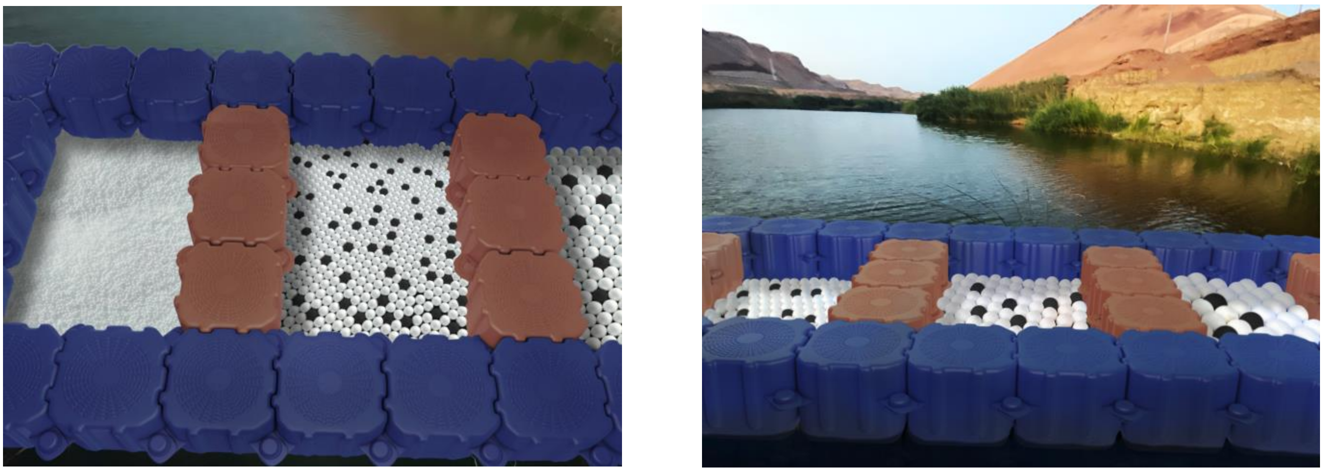

Figure 5. Wind and wave test layout.

Table 2. Wind and wave test design.

Fence No.	1	2	3	4	5
D (mm)	10	40	80	120	150
Covering rate (%)	90.1	89.4	88.3	87.3	85.6

The series specifications of a PE buoyancy tank were as follows: the dimensions were 500 × 500 × 400 mm, the weight of a single buoyancy tank was 7 ± 0.5 kg, and the fence area was 1.5 m^2. Table 2 shows the measured coverage of each fence.

The meteorological data came mainly from the FORAIN six-element weather station (Figure 6) installed onsite to realize all-weather recording of surface water temperature, wind speed, environmental humidity, and other data. Table 3 shows the specific monitoring items. When the weather station replaced the battery, the evaporation capacity was φ 20. The measured data from the evaporating dish were used as a supplement, and the wind speed data were supplemented by a COS-03 handheld weather station.

Table 3. Monitored items in the weather station.

Meteorological Elements	Measuring Range	Accuracy
Wind speed	0–70 m/s	0.1 m/s
Evaporation capacity	0–1000 mm	0.1 mm
Illumination	0–200,000 LUX	10 LUX
Net radiation	−2000–2000 W/m^2	1 W/m^2
Humidity	0–100% RH	0.1% RH
Water temperature	−50–100 °C	0.1 °C

Figure 6. Automatic weather station used in the test. Note: The meaning of Chinese in the figure includes brand of weather station, equipment name, corporate name, contact telephone and official website address.

4. Evaporator Test Results and Analysis

4.1. Calculation of Evaporation Inhibition Rate of Static Water Surface

When the wind speed was 0–0.2 m/s, the impact on the water surface and floating balls was very small. The water surface was calm, without fluctuation; the floating balls were relatively static, and the parts of the floating balls above the water surface were completely dry. At this time, water in the evaporator was only lost through the pores between the floating balls. The water loss in the evaporator when the wind speed was 0–0.2 m/s was regarded as the still water evaporation loss. The calm state often occurred at noon and in the early morning, and the evaporation rate varied. In order to calculate the average evaporation under the calm state, we took the hour (h) as the scale, took 150 h at noon and in the early morning from March to October, and measured the evaporation of six evaporators with the same water level measuring needle (Vernier accuracy of 0.1 mm). The measuring point was at the center of the water surface, and each water level data point was measured three times to take the average value. After the floating balls were laid, the evaporation capacity decreased by different degrees compared with that of the blank group. The ratio of the reduced evaporation capacity to the evaporation capacity of the blank group was the evaporation inhibition rate of the evaporator. The inhibition rates of still water evaporation under the coverage of floating balls of various diameters calculated via this method are shown in Table 4, where e_{d} is the diurnal evaporation, in mm; e_{n} is the evaporation at night, in mm; e is the total still water evaporation, in mm; i_{d} is the diurnal ESE, in %; i_{n} is the ESE at night, in %; i_0 is the average ESE in still water, in %; C_1 is the floating ball coverage in the evaporator (see Table 1), in %; and i_0 is the ESE when the coverage rate is 91%, calculated by the ratio method, and recorded as i.

Table 4. Calculation of evaporation inhibition rate in still water.

D (mm)	e_d (mm)	e_n (mm)	e (mm)	i_d (%)	i_n (%)	i_0 (%)	C_1 (%)	i (%)
10	16.05	4.15	16.58	70.3	78.5	74.4	88.2	76.8
40	9.21	3.75	13.01	86.4	84.3	85.8	86.1	90.7
80	11.43	4.14	15.57	83.4	82.6	83.1	84.5	89.5
120	12.04	4.54	16.58	82.8	81.0	81.9	83.4	89.4
150	12.48	4.65	17.13	82.1	80.5	81.3	83.2	88.9
No coverage	67.72	23.88	91.60	0.0	0.0	0.0	0	0.0

It can be seen from Table 4 that when the floating balls and water surface were not affected by wind and waves, the EPS floating balls with a diameter of 40 mm had the highest ESE of 85.5%; meanwhile, the 10 mm floating balls had the worst evaporation inhibition effect, because about half of the balls' volumes were below the water surface, and the water between the floating balls was subject to surface tension, resulting in the floating balls also having a high WR in the absence of wind, which accelerated water evaporation to a certain extent.

4.2. Calculation of Average Evaporation Inhibition Rate in Non-Freezing Period

At 20:00 every day, the water level of each evaporator was measured with the same water level measuring needle (vernier accuracy of 0.1 mm), and the measured cumulative evaporation of the evaporator covered by the floating ball of each diameter is shown in Figure 7. e_x is the evaporation capacity of each evaporator, in mm; e_0 is the evaporation capacity of the evaporator in the blank group, in mm.

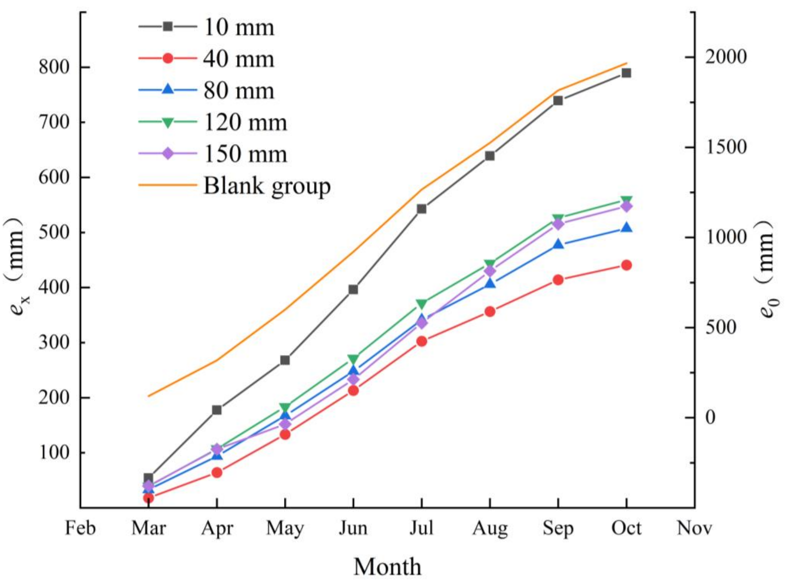

Figure 7. Cumulative evaporation capacities of all evaporators for different diameter balls.

ESE in evaporator (I_s) was calculated by a volume method, according to Formula (1):

$$I_s = 1 - e_x/e_0 \tag{1}$$

The monthly ESE was calculated from the monthly evaporation data, and the average ESE (I_1) in the non-freezing period was calculated with the sum of e_x and the sum of e_0. Table 5 shows the results, and Figure 8 shows the relationship between ESE and floating ball diameter.

Table 5. ESE of evaporator test by month.

Month	I_s (%)				
	***D* (mm)**				
	10	**40**	**80**	**120**	**150**
March	54.89	84.86	72.55	67.41	66.90
April	37.95	76.90	69.34	65.80	66.48
May	67.85	75.39	73.92	72.85	77.78
June	59.97	75.06	74.79	72.56	73.64
July	57.67	74.20	73.00	71.03	70.46
August	62.83	79.16	75.10	72.09	71.19
September	65.59	80.25	75.55	71.74	70.70
October	67.84	79.95	76.69	71.43	69.57
I_1 (%)	59.57	76.31	73.04	70.47	71.82

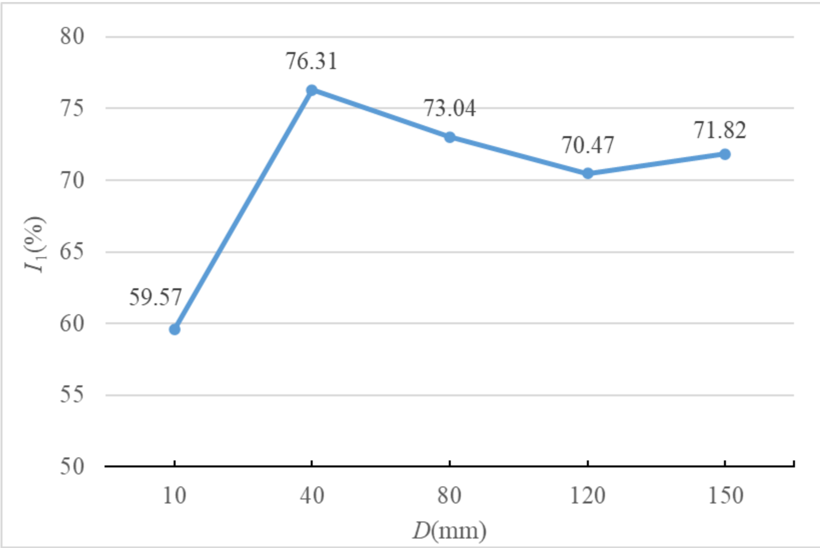

Figure 8. I_1–D diagram for the evaporator test.

It can be seen from the calculation results in Table 5 that among the five diameters of EPS floating balls, floating balls with a diameter of 40 mm had the highest ESE in each month, and in the whole non-freezing period.

It can be seen from Figure 8 that in the evaporator test, the relationship between the ESE and floating ball diameter is not a single function, and it is higher when the diameter is around 40 mm. Considering the impact of wind and waves, when laying in artificial ponds and reservoirs with low wind speed in the area, EPS floating balls with a diameter of 40–80 mm should be selected.

What needs to be added is that the specification of the evaporator was limited as the side wall of the evaporator weakened the influence of wind speed and waves on the internal floating balls. If the ambient wind speed is greater than 3 m/s, it is necessary to further prove the anti-evaporation effect of the floating ball on the water surface by using a larger evaporator or in the actual project when applying the floating ball to reduce evaporation in small-sized water bodies.

5. Wind and Wave Test Results and Analysis in the Reservoir Area

5.1. Wind Speed Data Analysis

The wind speed data were recorded by a COS-03 handheld weather station and a FORAIN weather station at the same time, and the recording interval of both methods was 10 min. The wind speed was analyzed by hour (h). The annual non-freezing period of the test area was from 3 March to 28 November 2022, a total of 270 days. The effective recording time was 6477 h, the wind speed durations and frequency (p) are shown in Table 6.

Table 6. Duration and frequency of wind speed at all levels during the non-freezing period.

Wind Speed (m·s^{-1})	Month									Duration (h)	p (%)
	March	April	May	June	July	August	September	October	November		
0–0.2	18	20	21	44	29	17	26	25	21	221	3.41
0.3–1.5	311	260	45	403	198	71	54	137	235	1714	26.46
1.6–3.3	316	244	501	201	163	195	315	478	359	2772	42.80
3.4–5.4	42	129	153	70	142	375	283	103	32	1329	20.52
5.5–7.9	3	30	24	2	114	76	39	1	2	291	4.49
8.0–10.7	2	17	0	0	57	10	3	0	0	89	1.37
10.8–13.8	0	12	0	0	21	0	0	0	0	33	0.51
13.9–17.1	0	8	0	0	14	0	0	0	0	22	0.34
>17.2	0	0	0	0	6	0	0	0	0	6	0.09
Total (h)		720	744	720	744	744	720	744	649	6477	100

It can be seen from Table 6 that the duration of level 2 wind accounted for 42.8% of the total recorded time, and the time of average wind speed at levels 1–3 (0.3–5.4 m·s^{-1}) accounted for 89.78% of the total recorded time. On a seasonal scale, the wind speed in spring and summer was relatively high, and the periods of high wind speed mainly occurred in April and July. The wind speed in autumn was low, the monthly average wind speed changed gently, and the wind speed change range was narrow. The maximum instantaneous wind speed during the non-freezing period was 18.16 m·s^{-1}, which was recorded on 30 September. Figure 9 shows the wind speed characteristics of each month.

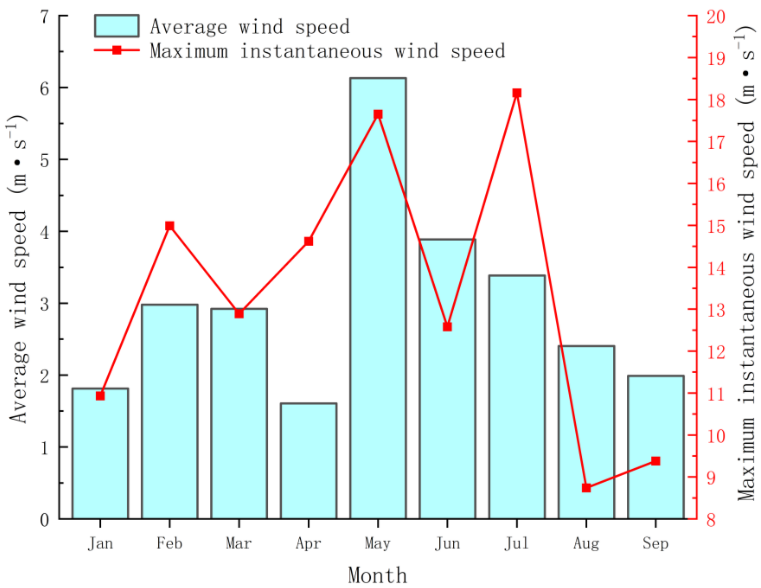

Figure 9. Wind speed characteristics of reservoirs in the test area.

In the process of data processing, it was found that on the day (d) scale, the most frequent windless state occurred at 2–6 A.M. The preliminary analysis showed that the surface was cooled by the release of long-wave radiation in the evening. When the surface temperature and the atmospheric temperature were close, the surface thermal radiation effect was the lowest, the atmospheric convection was the weakest, and the windless condition usually occurred at this time.

5.2. Calculation and Analysis of Wet Ratio

The wettability of floating balls under different wind speeds directly affected the anti-evaporation effect, and the wettability of floating balls was determined by means of dyeing. During the test, it was found that a certain brand of printer ink showed good adhesion to the EPS floating balls and had good water solubility after natural drying. After laying the dyed floating balls on the water for one hour, the fading edges were clear (Figure 10), and the product was used as a colorant.

Figure 10. Sample of EPS floating ball after dyeing and fading.

In order to reduce the negative impact on the environment, when measuring the WR, 10% of the floating balls in each buoyancy tank fence were selected for dying (Figure 3) and were then placed evenly into the buoyancy tank fence before timing was started. After one hour, they were removed and dried immediately. A Vernier caliper with an accuracy of 0.1 mm was used to measure the diameter of the bottom circle of the wetted ball crown on the spot, in order to calculate the WR of the floating balls. The WR of dyeing floats of each diameter were calculated, and the average value was taken as the average WR of the floats in the buoyancy tank at a specific wind speed. The wettability of the floating balls was calculated according to Formula (2):

$$\lambda = \frac{S_1}{S - S_2} \times 100\% \tag{2}$$

where: λ is the wet ratio (%); S_1 is the wetted area of the floating balls or buoyancy tank caused by wind and waves (cm^2), and the wetted area of the floating balls was calculated according to formula (3) of the surface area of the ball crown; S is the surface area of pontoon fence and floating ball (cm^2); and S_2 is the spherical crown surface area (cm^2) below the still water surface after the buoyancy tank or floating ball cover was paved, as shown in the shaded part of Figure 11.

$$S_1 = 2\pi Rh \tag{3}$$

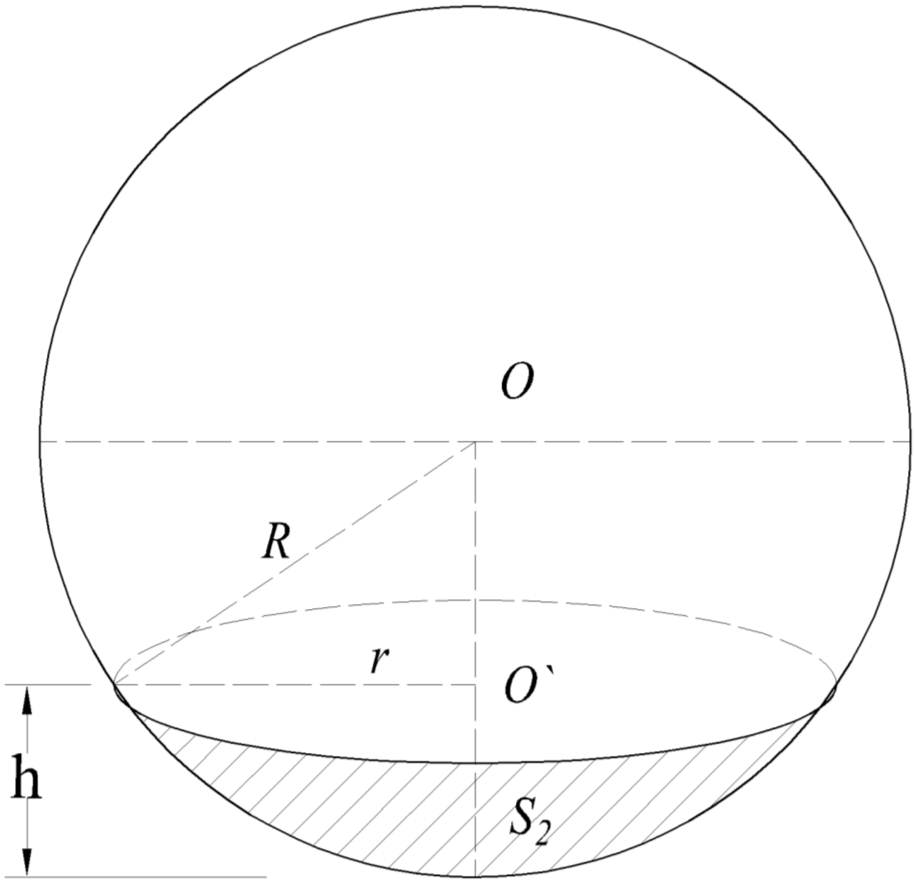

Figure 11. Schematic diagram of spherical crown calculation.

Here, R is the radius of floating balls (cm); h is the height of the wetted part (spherical cap), calculated according to Formula (4).

$$h = R - \left(R^2 - r^2\right)^{0.5} \tag{4}$$

where r is the circle radius of the spherical crown bottom surface of the wetted part (Figure 11), which was calculated by measuring the diameter of the spherical crown bottom surface with a Vernier caliper with an accuracy of 0.1 mm.

At each level of wind speed, the WR of each floating ball diameter was measured 10 times, and the average value was taken as the WR of the floating balls at all levels of wind speed. The above method was used to calculate the wettability of the EPS floating balls and buoyancy tank fence with different diameters under different wind speeds. The results are shown in Table 7.

In the test, it was found that when the EPS floating balls were closely arranged, there were six floating balls on the periphery of each floating ball to form a unit in the way of point contact. The friction between the floating balls was relatively large, which could play a role of mutual stability, and the stability effect was more obvious in the case of heavy wind and waves. With an increase in wind speed, the proportion of wetness caused by floating balls rolling in water decreased, and the proportion of wetness caused by wave splashing increased. Due to the small specific gravity of the material, the larger the diameter of the buoy, the smaller the proportion of the draft to the height of the buoy. Before the wave height reached the point where the buoy could submerge the whole buoy, the three kinds of buoys with a diameter of 80 mm and above swung up and down with the wave more synchronously. The wetting rate mostly came from the rotation of the buoy on the water surface. When the wave height was greater than the buoy diameter, the wetting rate increased significantly. The 10 mm floating ball was completely wet when the wind speed reached level 4 and basically lost its ability to prevent evaporation; the maximum average wetting rate of the 150 mm floating balls in the non-freezing period was only 36.6%. At the same wind speed, the wetting rate of the floating ball decreased with an increase in its diameter.

Table 7. Wet ratio of fence and floating balls at different wind speeds.

Wind Speed ($m \cdot s^{-1}$)	λ (%)				
	D (mm)				
	10	40	80	120	150
0–0.2	10	0	0	0	0
0.3–1.5	32	3.8	0	0	0
1.6–3.3	52	4.8	3.6	2.5	0
3.4–5.4	82	6.4	7.2	4.2	2.6
5.5–7.9	100	11.2	12.8	6.8	4.5
8.0–10.7	100	20.6	22.4	10.2	8.9
10.8–13.8	100	55	57.2	27.6	16.1
13.9–17.1	100	64.4	66.8	32.8	24.4
>17.2	100	76.6	64.2	48.6	36.6

5.3. ESE Calculation

In the wind wave test, the water evaporation loss included the loss through the pores between the floating balls, and the evaporation loss due to the wetting of the floating balls. It was assumed that all the water on the surface of the wet floating balls was lost through evaporation; that is, the WR was the water evaporation loss rate. This test mainly considered the influence of different wind speeds on the floating balls in the floating tank fence; the WR of the floating balls is a variable, and the ESE of the floating balls is calculated according to Formula (5):

$$I_w = 1 - \lambda i - i_9 \tag{5}$$

Where: I_w is the ESE of the floating balls, in %; λ is the wettability of floating balls under the action of wind and waves (Table 7), in %; i is the ESE when the coverage rate of floating balls of each diameter is 91% in still water, with the value taken from Table 4; and i_9 is the evaporation loss rate corresponding to 9% of the pores between the floating balls, in %, calculated according to Formula (6).

$$i_9 = 1 - i \tag{6}$$

The average ESE of the wind wave test (I_2) was calculated according to Formula (7):

$$I_2 = \sum p \cdot I_w \tag{7}$$

where p is the frequency of the wind speed at different levels.

The ESEs of the floating ball covers in the wind wave test were calculated by Formulas (4)–(6), as shown in Table 8.

It can be seen from Table 8 that in the wind and wave test in the reservoir area, the ESE of the 10 mm floating balls was the lowest, only 34.79%, and the ESEs of the other four diameters of floating balls were all above 85%, and increased with diameter. Under the condition of high wind speed, the use of larger diameter floating balls achieved a better evaporation inhibition effect, but the larger diameter floating balls correspond to higher material costs, and the actual application should be analyzed according to local meteorological conditions. In Turpan, it is recommended to use floating balls with a diameter of 40–80 mm, since they have a better anti-evaporation effect and are more economical.

Table 8. ESEs of fence and floating balls at different wind speeds.

Wind Speed ($m{\cdot}s^{-1}$)	p (%)	I_w (%)				
		D (mm)				
		10	40	80	120	150
0–0.2	3.41	2.36	3.09	3.05	3.05	3.03
0.3–1.5	26.46	13.82	23.09	23.68	23.66	23.53
1.6–3.3	42.80	15.78	36.95	38.30	37.30	38.05
3.4–5.4	20.52	2.84	17.42	17.04	17.57	17.77
5.5–7.9	4.49	0.00	3.62	3.51	3.74	3.81
8.0–10.7	1.37	0.00	0.99	0.95	1.10	1.11
10.8–13.8	0.51	0.00	0.21	0.20	0.33	0.38
13.9–17.1	0.34	0.00	0.11	0.10	0.20	0.23
>17.2	0.09	0.00	0.02	0.03	0.04	0.05
I_2 (%)	-	34.79	85.50	86.87	87.01	87.96

5.4. Determination of the Wind Speed at Which the Floating Balls Were Blown out of the Fence (V_{out})

Since the density of EPS floating balls is low (18 kg/m^3), in order to ensure that the floating balls are easy to maintain after being laid in a large area to have the effect of preventing evaporation for several years, the floating balls should not be blown out of the buoyancy tank fence by the wind under the conditions of wind and waves; this was difficult to prevent in the actual project. The correlation between the coverage rate and water saving rate of PE floating balls in still water showed that when the coverage rate of PE floating balls was 75%, the corresponding ESE was only about 60%. In fact, under the conditions of wind and waves, the floating balls were in a non-compact arrangement with 75% coverage, the binding force was weak, and the corresponding ESE was lower. In this test, the instantaneous wind speed at which the floating balls were blown away from the buoyancy tank fence was regarded as the blowing wind speed (V_{out}, $m{\cdot}s^{-1}$) of the floating balls. After the average wind speed on the water surface reached or exceeded the blowing wind speed and lasted for a certain time, the floating balls were blown away from the buoyancy tank in succession. When the coverage rate of the floating balls in a single buoyancy tank fence was less than 75%, it was considered that the floating balls in the buoyancy tank fence lost their anti-evaporation ability; that is, the anti-evaporation structure was damaged The time from the floating balls being blown out of the fence to the structural damage was recorded as the damage duration ($\bar{t}_d$, min). In the non-freezing period, the blowing wind speed and the number of damages (T) to the floating balls of each diameter were measured to determine the applicability of the EPS floating balls under the action of continuous wind and waves. The results are shown in Table 9.

Table 9. The wind speed at which the floating balls were blown out of the fence.

Items	D (mm)				
	10	40	80	120	150
V_{out} ($m{\cdot}s^{-1}$)	13.6	12.2	13.8	14.6	16.2
$\bar{t}_d$ (min)	94 *	88	79.5	73.3	68
T	1	1	2	2	1

Note: It was difficult to accurately calculate the coverage rate of the 10 mm floating balls in the fence in Table 9. $\bar{t}_d$ is the artificial observation duration; data marked with * in the table has a certain error compared to the actual damage duration.

During the test, it was found that the small diameter floating balls were more likely to be damaged under the conditions of strong wind and waves; moreover, the damage lasted longer. Large-diameter floating balls were not as easy to blow out of the fence, but the damage duration was short; that is, the diameter of the floating balls was inversely proportional to the average damage duration. Taking the 80 mm and 150 mm floating balls as an example, the fence area was 1.5 m^2, and the numbers of floating balls blown away when the structure was damaged were 60 and 17, respectively. After the floating balls in the fence were blown away from the fence, the collision, rolling and stacking of the remaining floating balls in the fence became more serious. Collision and rolling led to a sudden increase in the wetting rate of the floating balls, which consequently lost friction and static power compared to the original adjacent floating balls after being superimposed. It became easier for them to be rolled and blown out of the fence, indicating that the actual application of the EPS floating balls in the reservoir area depends on the restraint effect of the buoyancy tank fence. To prevent the destruction of the anti-evaporation structure, another plastic net could be covered and fixed at the bolt connection at the four corners of the fence.

5.5. Durability Analysis of EPS Floating Balls

The applicability of EPS material as anti-evaporation floating balls was judged by counting the numbers of damaged floating balls during the test. After two months of the freezing test and ten months of the hydrostatic test, the same batch of test balls underwent 12 months of hydrostatic testing, and 0.16% of the balls were significantly deformed and peeled due to the freeze–thaw effect, while 0.44% of the balls were damaged due to light, wetting, and weathering, with a total damage rate of about 0.6%. After oxidation and discoloration, there was no obvious impact on the anti-evaporation performance. Figure 12 shows common damage patterns.

Figure 12. Common failure modes of EPS balls.

5.6. Economic Analysis

Since the test used solid floating balls, the size of the floating balls determined the consumption of raw materials, and also determined the cost of the scheme. The coverage rate was 91% when the spheres are flat on the water surface and in close arrangement. At this time, the projected area of floating balls on the water surface in a 1 m^2 water area was 0.91 m^2, and the number of floating balls required to cover each square meter of surface (N) was calculated based on this area. After consulting several manufacturers, the average purchase unit prices of five floating ball diameters were obtained, and the calculated laying costs per square meter are shown in Table 10.

Table 10. Preliminary calculations of floating ball costs.

D (mm)	Surface Area (m^2)	N (pcs)	Unit Price (CNY)	Total (CNY)
10	7.9×10^{-5}	11587	0.007	81.11
40	1.26×10^{-3}	725	0.056	40.60
80	5.03×10^{-3}	182	0.28	50.96
120	1.13×10^{-2}	80.5	1.23	99.02
150	1.77×10^{-2}	51.4	2.3	118.22

From Table 10, 40 mm and 80 mm floating balls are more economical. It is recommended to use 40 mm diameter floating balls without protection to reduce maintenance costs.

6. Conclusions

In contrast to the test in the still water evaporator, the factor of wind and waves cannot be ignored when the floating balls are arranged in the reservoir. This test takes the wind speed as the entry point and studies the effect of EPS floating ball coverings on the evaporation inhibition of the reservoir water surface. As an environmentally friendly material, the recycling significance of EPS material is considerable [22–24]. In areas with more special climatic conditions, or in reservoirs with more complex water quality and chemical composition, an antioxidant based on organosilicon and fluoropolymer can be added, or coatings with cross-linkable polymer adhesive can be used, which can enhance the anti-ultraviolet damage and weathering ability of the floating balls, making them more durable [25–27], helping them maintain stability for many years under outdoor conditions, and further reducing the overall costs of the project. In this test, only 1.5 m^2 of fence area was used. If the structure were arranged in the reservoir, the price of a buoyancy tank would account for more than 80% of the total project cost. In practical application, while ensuring the ESE, the use of a larger fence area should be considered in order to ensure the economy of the scheme. Among the most important results reached are the following:

- The outdoor evaporator test showed that the white EPS floating balls can significantly inhibit evaporation, especially in summer; the ESE of EPS floating ball reached 76.31% in the non-freezing period, which was greater than 70.6% in the non-freezing period of 100 mm PE floating balls [9]. It is better to use EPS floating balls with diameters of 40 mm to suppress water evaporation for artificial ponds or small reservoirs in arid areas with low wind speed.
- In the buoyancy tank fence with an area of 1.5 m^2, the average ESE was above 85%, except for the 10 mm floating balls, and the anti-evaporation effect was excellent. The average ESE of EPS floating balls with a diameter of 150 mm in the whole non-freezing period reached 88.85%, which was the highest among the five kinds of floating balls. Floating ball diameters of 40–80 mm have more economic advantages in a reservoir.
- During the test, only a few floating balls did not have extrusion deformation and individual damage; the floating balls of all diameters met the strength requirements. Under the condition of high wind speed, additional protective measures, such as woven mesh and plastic mesh, can be considered to prevent the floating balls from losing their anti-evaporation effect as a result of being blown out of the fence.

Author Contributions: Conceptualization, B.W. and K.S.; data curation, B.W. and S.X.; formal analysis, B.W. and K.S.; investigation, S.X. and J.W.; methodology, K.S. and B.W.; project administration, K.S. and B.W.; resources, B.W. and G.Z.; data curation, B.W.; writing—original draft preparation, B.W.; writing—review and editing, K.S.; visualization, B.W.; supervision, K.S. All authors have read and agreed to the published version of the manuscript.

Funding: This research received no external funding.

Data Availability Statement: All data are available from the first author on reasonable request.

Conflicts of Interest: The authors declare no conflict of interest.

References

1. Xie, R.-H.; Wang, A.-H.; Hua, W. Temporal and Spatial Distribution Characteristics and Influencing Factors of Pan Evaporation in China from 1961 to 2013. *Clim. Environ. Res.* **2020**, *25*, 483–498. [CrossRef]
2. Jiang, H.-B.; Tang, K.; He, X.-L. Experimental study on inhibiting water surface evaporation of reservoir in arid region. *J. Arid. Land Resour. Environ.* **2016**, *30*, 119–124. [CrossRef]
3. Tian, W.; Liu, X.; Wang, K.; Bai, P.; Liu, C. Estimation of reservoir evaporation losses for China. *J. Hydrol.* **2021**, *596*, 126142. [CrossRef]
4. Yue, C.F.; Shi, K.B.; Cao, W. Analysis of advantages and disadvantages of water resources development mode in Xinjiang. *J. Water Saving Irrigation. J.* **2014**, *7*, 60–62.

5. Cao, X.C.; Yang, C.Y.; He, X.; Shi, H.D.; Shu, R.; Zheng, Y.L.; Wang, Z.C.; Guo, X.P. Assessing the Spatial Variation of rrigation Water Use Efficiency in Grain Production of China. *J. China Rural Water Hydropower* **2016**, *8*, 128–132. [CrossRef]
6. Jiang, Q.F.; Zhang, Y. Analysis of current situation and development countermeasures of agricultural water-saving irrigation in China. *J. Haihe Water Resour.* **2022**, *5*, 1–4. [CrossRef]
7. Zhao, G. Estimating reservoir evaporation losses for the United States: Fusing remote sensing and modeling approaches. *Remote Sens. Environ. Interdiscip. J.* **2019**, *226*, 109–124. [CrossRef]
8. Bozorg-Haddad, O.; Yari, P.; Delpasand, M.; Chu, X. Reservoir operation under influence of the joint uncertainty of inflow and evaporation. *Environ. Dev. Sustain.* **2022**, *24*, 2914–2940. [CrossRef]
9. Abdelgaied, M.; Kabeel, A.E.; Zeleňáková, M.; Abd-Elhamid, H.F. Photovoltaic Plants as an Effective Option to Reduce Water Evaporation in Water-Stressed Regions and Produce Electricity: A Case Study of Lake Nasser, Egypt. *Water* **2023**, *15*, 635. [CrossRef]
10. Zahedi, R.; Ranjbaran, P.; Gharehpetian, G.B.; Mohammadi, F.; Ahmadiahangar, R. Cleaning of Floating Photovoltaic Systems: A Critical Review on Approaches from Technical and Economic Perspectives. *Energies* **2021**, *14*, 2018. [CrossRef]
11. Al-Widyan, M.; Khasawneh, M.; Abu-Dalo, M. Potential of Floating Photovoltaic Technology and Their Effects on Energy Output, Water Quality and Supply in Jordan. *Energies* **2021**, *14*, 8417. [CrossRef]
12. Juárez, M.L.A.; Ignacio, M.F.H.; Silvestre, S.L.R.; Romero, J.O.; Elizondo, E.C. Evaluation of the capacity of PET bottles, water aeration, and water recirculation to reduce evaporation in containers of water. *J. King Saud Univ.-Sci.* **2022**, *34*, 102046. [CrossRef]
13. Hou, Z.; Yan, X.; Li, X.; Han, K. Experimental Study on the Sensitivity of Floating Ball Parameters to Inhibition of Surface Evaporation. *Water Resources Power* **2018**, *36*, 27–29+33. Available online: https://kns.cnki.net/kcms2/article/abstract?v=qyszBj78zeI9raO8cjiFAq87rx77m-fy1m5GsUHNUcBfU4uWuer-R3tpok-f9exLI1KmbWoLyIKMigipl4tRkcqj0bEr0vAJX0xtNfWiYpEFZ4wPOu-uU_3-R83jgS8x&uniplatform=NZKPT&language=EN (accessed on 2 June 2022).
14. Li, C.L.; Shi, K.B.; Yan, X.J.; Jiang, C.-L. Experimental Analysis of Water Evaporation Inhibition of Plain Reservoirs in Inland Arid Area with Light Floating Balls and Floating Plates in Xinjiang, China. *J. Hydrol. Eng.* **2021**, *26*, 04020060. [CrossRef]
15. Shalaby Maram, M.; Nassar Ibrahim, N.; Abdallah Ahmed, M. Evaporation suppression from open water surface using various floating covers with consideration of water ecology. *J. Hydrol.* **2021**, *598*, 126482. [CrossRef]
16. Wuernisha, M.; Mayilaka, K. Analysis on Characteristics of Precipitation Variation in Gaochang District of Turpan City in Recent 39 Years. *Clim. Chang. Res. Lett.* **2021**, *10*, 5. [CrossRef]
17. Li, C.-L. Experimental Study on Water Evaporation and Water-saving of PVC Floating Plate and Floating Ball in the Plain Reservoir of Arid Area. Master's Thesis, Xinjiang Agricultural University, Xinjiang, China, 2016.
18. Meftah, R.; Van Stappen, J.; Berger, S.; Jacqus, G.; Laluet, J.-Y.; Guering, P.-H.; Van Hoorebeke, L.; Cnudde, V. X-ray Computed Tomography for Characterization of Expanded Polystyrene (EPS) Foam. *Materials* **2019**, *12*, 1944. [CrossRef] [PubMed]
19. Bae, M.; Ahn, H.; Kang, J.; Choi, G.; Choi, H. Determination of the Long-Term Thermal Performance of Foam Insulation Materials through Heat and Slicing Acceleration. *Polymers* **2022**, *14*, 4926. [CrossRef]
20. Yartsev, V.P.; Andrianov, K.A. Effect of Aggressive Liquid Media on the Durability of Polystyrene foam under Load. *Int. Polym. Sci. Technol.* **2003**, *30*, 22–25. [CrossRef]
21. Feng, Q. Analysis of evaporation from large water bodies in Xinjiang. *Water Conserv. Sci. Technol. Econ.* **2015**, *21*, 2.
22. Sow, P.K.; Singhal, R. Sustainable approach to recycle waste polystyrene to high-value submicron fibers using solution blow spinning and application towards oil-water separation. *J. Environ. Chem. Eng.* **2020**, *8*, 102786. [CrossRef]
23. Cirisano, F.; Ferrari, M. Superhydrophobicity and Durability in Recyclable Polymers Coating. *Sustainability* **2021**, *13*, 8244. [CrossRef]
24. Voith, K.; Spisák, B.; Petrik, M.; Szamosi, Z.; Szepesi, G.L. Non-Conventional Reinforced EPS and Its Numerical Examination. *Processes* **2023**, *11*, 12. [CrossRef]
25. Wang, W.; Sosa, J.M.; Knoeppel, D.W. Use of Polar Additives for Enhancing Blowing Agent Solubility in Polystyrene. U.S. Patent 20120208913A1. 16 August 2012. Available online: https://worldwide.espacenet.com/patent/search?q=pn%3DUS2012208913A1 (accessed on 4 February 2023).
26. Ying, C.H. Foaming Additive Agent, Formulation of Open-Cell Microcellular Polystyrene Foam, Open-Cell Microcellular Polystyrene Foam and Method for Making Thereof. Patent TWI339667(B). 1 April 2011. Available online: https://kns.cnki.net/kcms2/article/abstract?v=qyszBj78zeKgJrXfK0BqHw5o3_eneb9LzlsSVYJZhUxjC7CWE9TnNnoGBPMBGOvg6Tmai6HNpEXvN59K0OsgPvGB1KzncQWQMUpoLPM5ut9cMHx9iHPmfw==&uniplatform=NZKPT&language=EN (accessed on 2 February 2023).
27. Andrianov, K.A.; Yartsev, V.P. Influence Of Composition On The Strength, Durability And Thermal Stability Of Polystyrene Foam. *Trans. Tambov State Tech. Univ.* **2002**, *8*, 331–335.